Article

Discovery Medicine 2025; 37(202): 2637–2648
https://doi.org/10.24976/Discov.Med.202537202.221

ADRB2 Overexpression Reverses Plasma Gelsolin-Induced TGF-β1 Upregulation in Mesangial Cells of IgA Nephropathy

Changsong Han[1], Yujiang Chen[1], Kun Wang[1], Chunlin Chen[1], Mao Yang[1], Chuanhui Sun[2,*]

[1]Department of Pathology, The First Affiliated Hospital of Guizhou University of Traditional Chinese Medicine, 550001 Guiyang, Guizhou, China
[2]Department of Otorhinolaryngology, Head and Neck Surgery, The First Affiliated Hospital of Guizhou University of Traditional Chinese Medicine, 550001 Guiyang, Guizhou, China
*Correspondence: chuanhuisun0803@163.com (Chuanhui Sun)
Submitted: 18 July 2025 Revised: 24 September 2025 Accepted: 29 September 2025 Published: 20 November 2025

Background: IgA nephropathy (IgAN), a common glomerulonephritis, is characterized by glomerular deposition of IgA-containing immune complexes, which drive mesangial cell proliferation and extracellular matrix synthesis through transforming growth factor beta 1 (*TGF-β1*) overexpression. Previous studies demonstrated abundant plasma gelsolin (pGSN) deposition in IgAN glomeruli, which promoted *TGF-β1* expression. However, the molecular mechanisms by which pGSN modulates *TGF-β1*-mediated fibrosis in mesangial cells remain unclear. This study aimed to elucidate these mechanisms and identify potential therapeutic targets for inhibiting glomerular fibrosis in IgAN.

Methods: Human glomerular mesangial cells (HMCs) were stimulated with pGSN. Transcriptome sequencing was applied to screen for key regulators of *TGF-β1*. Identified factors and *TGF-β1* expression were validated by quantitative polymerase chain reaction (qPCR), western blot (WB), and immunofluorescence (IF). The functional role of the candidate regulator, adrenoceptor beta 2 (*ADRB2*), was further investigated using protein–protein interaction prediction and *ADRB2* overexpression assays, including under co-stimulation with polymeric IgA1 (pIgA1).

Results: Transcriptome sequencing revealed the cyclic adenosine monophosphate (cAMP) pathway gene *ADRB2* as a potential fibrosis regulator. Stimulation of HMCs with pGSN reduced *ADRB2* ($p < 0.01$) and cAMP dependent protein kinase (*PKA*) ($p < 0.01$) expression, while significantly increasing *TGF-β1* ($p < 0.001$). Conversely, *ADRB2* overexpression increased *ADRB2* ($p < 0.001$) and *PKA* ($p < 0.001$) levels while decreasing *TGF-β1* ($p < 0.001$). Notably, *ADRB2* overexpression reversed the *TGF-β1* upregulation induced by combined pGSN and pIgA1 stimulation.

Conclusion: pGSN synergizes with pIgA1 to enhance *TGF-β1* expression and glomerular fibrosis in IgAN by suppressing the *ADRB2*/cAMP signaling pathway. *ADRB2* may represent a promising therapeutic target for antifibrotic strategies in IgAN.

Keywords: pGSN; cAMP signaling; ADRB2; TGF-β1; fibrosis

Introduction

IgA nephropathy (IgAN) is one of the most prevalent primary glomerulonephritides, characterized by distinctive pathological features, including galactose-deficient polymeric IgA1 (pIgA1) deposition in the glomerular mesangium, mesangial cell proliferation, and glomerular sclerosis with fibrosis [1,2]. A subset of patients progresses to end-stage renal disease (ESRD) within 20–30 years, often accompanied by glomerulosclerosis and fibrosis. Clinical studies have demonstrated that the severity of glomerulosclerosis correlates significantly with an elevated risk of adverse renal outcomes, including serum creatinine doubling and progression to ESRD [3–5]. Furthermore, the Oxford Classification of IgAN identifies segmental glomerulosclerosis (S lesion) as an independent prognostic indicator of renal survival [6,7]. Glomerular fibrosis represents an early stage in the development of glomerulosclerosis [8], elucidating the molecular mechanisms underlying glomerular fibrosis is therefore critical for designing preventive strategies and early interventions to mitigate ESRD progression in IgAN patients.

Endothelial-to-mesenchymal transition (EMT) in glomerular endothelial cells constitutes a principal cause of glomerular fibrosis. This process is regulated by multiple signaling pathways, including the transforming growth factor beta (TGF-β) pathway, Wnt/β-catenin, and nuclear factor kappa B (NF-κB) pathways [9–11]. Among these, the TGF-β signaling pathway plays a predominant regulatory role, with *TGF-β1* serving as a crucial molecular driver of fibrotic progression [12,13].

Plasma gelsolin (pGSN) was first discovered by Yin and Stossel [14] in rabbit lung macrophages in 1979, where it was shown to regulate actin remodeling in a calcium-

dependent manner, promoting interconversion between the cytoplasmic gel and sol state. In healthy humans and other mammals, serum pGSN concentrations typically range from 200 ± 50 mg/L [15]. Numerous studies have reported decreased serum pGSN levels in diverse pathological conditions, including bacterial sepsis, trauma, idiopathic lung injury, acute liver injury, and allogeneic hepatocyte transplantation [16–21]. Based on these findings, our group examined pGSN in several types of glomerulonephritis for the first time. Preliminary experiments revealed that serum pGSN concentrations were significantly reduced in IgAN patients, while deposition was observed within glomeruli [22]. Our initial findings suggest that pGSN may play a crucial role in the pathogenesis and progression of IgAN. Furthermore, we demonstrated that pIgA1 synergizes with pGSN to enhance *TGF-β1* expression in human mesangial cells (HMCs) [23].

TGF-β1 is a key molecular mediator of glomerulosclerosis. Upon binding to the TGF-β receptor type II (TβRII) on HMCs, it activates the *Smad2/3* complex, which subsequently associates with Smad4 to form a heterotrimeric complex. This complex translocates to the nucleus, where it promotes transcription of fibrosis-related genes such as collagen type I alpha 1 chain (*COL1A1*), connective tissue growth factor (*CTGF*), and plasminogen activator inhibitor 1 (*PAI-1*), thereby exacerbating glomerulosclerosis [24–26]. Notably, adrenoceptor beta 2 (*ADRB2*) serves as an antifibrotic regulator, exhibiting protective effects against fibrosis in the lung [27], bladder [28], and human dermal fibroblasts [29]. However, the specific contribution of *ADRB2* to glomerular fibrosis and its potential interaction with pGSN remain unclear.

To further investigate the regulatory interplay between pGSN and *TGF-β1*, and to determine whether *ADRB2* mediates this process, HMCs were stimulated with pGSN, followed by transcriptome sequencing to identify differentially expressed candidate genes. Functional validation was performed using gene knockdown or overexpression approaches. Building on previous findings [23], this study demonstrates for the first time that pGSN and pIgA1 synergistically regulate glomerular fibrosis through the *ADRB2*/cyclic adenosine monophosphate (cAMP) signaling axis. These results expand the understanding of the pGSN-pIgA1 regulatory network and identify *ADRB2* as a novel molecular hub in IgAN fibrosis, providing valuable mechanistic insights and potential therapeutic targets.

Materials and Methods

Cell Culture and Treatment

Human mesangial cells (HMCs; MZ-1239, Mingzhoubio, Ningbo, China; STR authentication results provided in the **Supplementary Materials 1**) were routinely tested for mycoplasma contamination using 16S rRNA PCR (see **Supplementary Materials 2**) and confirmed negative. Cells were cultured in DMEM (C11995500BT, Gibco, Waltham, MA, USA) complete medium supplemented with 10% fetal bovine serum (AC03L055, Life-iLab, Shanghai, China) and 1% penicillin-streptomycin (C0222, Beyotime, Shanghai, China) at 37 °C in 5% CO_2. All experiments were performed using HMCs derived from the same biological source and maintained at passages 3–6. When the cell confluence reached 80–90%, cells were digested with pancreatin (S310KJ, BasalMedia, Shanghai, China), adjusted to a density of 2×10^5/mL, and seeded into 6-well plates at 2 mL per well. After adherence, the cells were cultured in the following groups: ① Normal HMCs group (Control): maintained in DMEM complete medium; ② pGSN stimulation group (pGSN): cultured in DMEM complete medium containing 10 μg/mL pGSN (HPG6-A, Cytoskeleton, Denver, CO, USA). After re-culturing each group for 48 hours, samples were harvested for subsequent experiments.

Quantitative Polymerase Chain Reaction (qPCR)

Total RNA was extracted using Trizol (CW0580S, Cwbio, Taizhou, China), and RNA concentration and purity were determined with a spectrophotometer (NanoDrop One/One C, Thermo Fisher, Waltham, MA, USA). Samples with OD_{260}/OD_{280} ratios of 1.8–2.1 were used for downstream analyses. cDNA synthesis was performed following the manufacturer's guidelines (TSK302M, Tsingke, Beijing, China). qPCR reactions were prepared with 2 × TSINGKE Master Mix (Green) (TSE002, Tsingke Biotechnology, Beijing, China) using cDNA as the template and run on a real-time PCR system (IQ5, Bio-Rad, Hercules, CA, USA). Relative mRNA levels were quantified using the $2^{-\Delta\Delta Cq}$ method, representing the fold changes in gene expression in treatment groups relative to controls. Primer sequences are listed in Table 1.

Table 1. Primer sequences for target genes.

Primer names	Sequences
TGF-β1-F	TACCTGAACCCGTGTTGCTC
TGF-β1-R	CCGGTAGTGAACCCGTTGAT
ADRB2-F	TTGCCTCTTCCATCGTGTCC
ADRB2-R	CCACCTGGCTAAGGTTCTGG
PKA-F	GCCTATGGCGTCCTGTTGTATG
PKA-R	GAAACAGCCTCCTTGGACAAGG
GAPDH-F	TCAAGGCTGAGAACGGGAAG
GAPDH-R	TCGCCCCACTTGATTTTGGA

TGF-β1, transforming growth factor beta 1; *ADRB2*, adrenoceptor beta 2; *PKA*, cAMP dependent protein kinase; *GAPDH*, glyceraldehyde-3-phosphate dehydrogenase.

Western Blot (WB)

Protein samples were extracted from cells collected in 1.5 mL centrifuge tubes using RIPA buffer (p0013B, Beyotime, Shanghai, China) supplemented with PMSF (P1045, Beyotime, Shanghai, China). Lysates were mixed with 5 × SDS loading buffer (8015011, Dakewei, Beijing, China) and separated by 10% SDS-PAGE gel (PG212, Yamei, Shanghai, China). Protein bands were transferred to PVDF membranes (10600023, Amersham, Germany), blocked, and incubated with primary antibodies overnight at 4 ℃. After washing, membranes were incubated with secondary antibody HRP-conjugated goat anti-rabbit IgG (H + L) (1:10,000, AS014, Abclonal, Wuhan, China) for 1 hour, followed by luminescence detection with ECL Plus (Amersham Pharmacia Biotech, Uppsala, Sweden). Protein bands were visualized using a gel imaging system (Universal Hood II, Bio-Rad, Hercules, CA, USA), and band intensities were quantified with ImageJ software (NIH, Bethesda, Bethesda, MD, USA).

Primary antibodies included: GAPDH (1:100,000, A19056, Abclonal, Wuhan, China), *TGF-β1* (1:1000, A2124, Abclonal, Wuhan, China), *ADRB2* (1:1000, A2048, Abclonal, Wuhan, China), and *PKA* (1:1000, PA5-67660, Thermo Fisher, Shanghai, China).

Transcriptome Sequencing Analysis

Three samples were selected from the control group and the pGSN group. Total RNA was extracted using Trizol, and its integrity and concentration were assessed with an Agilent 2100 Bioanalyzer (Agilent, Santa Clara, CA, USA). After quality control testing, sequencing libraries were constructed. Differentially expressed genes (DEGs) between the control and pGSN groups were analyzed using DESeq2 software (version 1.48.2; Bioconductor Project, Seattle, WA, USA). DEGs were defined as those with $p < 0.05$ and $|\log_2 \text{FoldChange}| > 1$. Identified DEGs were subjected to GO and KEGG enrichment analyses using ClusterProfiler. Library construction and transcriptome sequencing were performed on the Illumina sequencing platform (Novogene Co., Ltd.).

Vector Construction

The *ADRB2* sequence (NCBI Reference Sequence: NM_000024.6) was synthesized into the pLVX-IRES-puro vector (VT1464, YouBio, Hunan, China) at the EcoRI–BamHI cloning site. Complete sequence information is provided in **Supplementary Materials 3** (Sequence of *ADRB2*). The recombinant plasmid, following quality verification, was transformed into DH5α competent cells (B528413, Sangon Biotech, Shanghai, China). Positive antibiotic-resistant monoclonal colonies were selected for amplification, plasmids were extracted using the GoldHi EndoFree Plasmid Midi Kit (CW2581S, cwbiotech), and stored at –20 °C after quality inspection.

Cell Transfection

HMCs were seeded at 5×10^6 cells per dish and cultured in fresh 10 mL DMEM medium after 24 hours. The overexpression empty vector and the *ADRB2* overexpression plasmid were transfected into HMCs using the PEI MAX transfection reagent (24765-1, Polysciences, Niles, IL, USA). Six hours post-transfection, cells were assigned to the following groups: (i) Control; (ii) pGSN stimulation; (iii) pGSN + oe-NC, in which cells transfected with the empty vector were cultured in DMEM complete medium containing 10 μg/mL plasma gelsolin; (iv) pGSN + oe-*ADRB2*, in which cells transfected with the *ADRB2* overexpression plasmid were cultured in DMEM complete medium supplemented with 10 μg/mL plasma gelsolin. After 48 hours of incubation for each group, cells were harvested for subsequent experiments.

Immunofluorescence (IF)

Cell slides were fixed and permeabilized with 0.3% Triton X-100 solution (ST795, Beyotime, Shanghai, China) for 5 minutes at room temperature. Following PBS rinsing (G0002, Servicebio, Wuhan, China), slides were blocked with goat serum (C0265, Beyotime, Shanghai, China) for 30 minutes. Without additional washing, slides were incubated with primary antibody against *TGF-β1* (1:200, YT4632, ImmunoWay, TX, USA) at 4 ℃ for 16 hours, followed by secondary antibody CoraLite488-conjugated goat anti-rabbit IgG (H + L) (1:500, SA00013-2, Proteintech, Chicago, IL, USA) at room temperature for 1.5 hours. Nuclei were counterstained with DAPI (C1005, Beyotime, Shanghai, China) at room temperature for 5 minutes. Finally, slides were mounted with anti-fade medium (P0126, Beyotime, Shanghai, China) for microscopic examination. After DAPI staining, nuclei appeared blue, while positive fluorescence was visualized as green. Quantification of immunofluorescence was performed using ImageJ, measuring the mean fluorescence intensity with ROI-based background subtraction and consistent acquisition settings.

Extraction of pIgA1

Peripheral blood samples were collected from patients with primary IgAN at the First Affiliated Hospital of Guizhou University of Traditional Chinese Medicine between March 1, 2023, and November 30, 2023. Inclusion criteria for the IgAN group were: (1) biopsy-confirmed primary IgAN; (2) age 18–70 years; (3) no clinically significant hepatic or renal dysfunction; (4) no prior treatment with glucocorticoids or immunosuppressive agents; and (5) no active mucosal infection. Twenty-one IgAN patients meeting these criteria were enrolled. Exclusion criteria included failure to meet any of the above conditions. All participants provided written informed consent, and the study was approved by the Ethics Committee of Guizhou University of Traditional Chinese Medicine (approval No. KS2022-10).

For each patient, 20 mL of peripheral blood was drawn and centrifuged at 3000 r/min for 15 minutes. The supernatant was diluted with PBS (1:1) and centrifuged for 5 minutes. Two milliliters of the centrifuged supernatant were immobilized on cross-linked 4% agarose beads (R-200, Gold Biotechnology, St. Louis, MO, USA) in a Jacalin affinity column and incubated for 30 minutes. Columns were washed with 175 mM Tris-HCl (pH 7.4) until the optical density (OD) at 280 nm dropped below 0.10. Elution was performed using 175 mM Tris-HCI containing 0.1 M melibiose (B20866, Yuanye, Shanghai, China) in 3.0 mL fractions until OD returned to 0.1. Jacalin-binding proteins were further purified by molecular sieve chromatography using a Sephacryl S-200 HR column (2.0 × 57 cm, Pharmacia Biotech, Inc., Piscataway, NJ, USA). The Pharmacia Intelligent System with Micro Peak Detector (Pharmacia Biotech, Uppsala, Sweden) was applied to obtain 2 mg/mL samples. The Sephacryl S-200 HR column generated three absorption peaks at OD 280 nm, corresponding to pIgA1, monomeric IgA1 (mIgA1), and additional heteroproteins. The pIgA1 concentration was determined using a BCA kit (P0012, Beyotime, China).

HMCs were seeded at a density of 2×10^5 cells/mL in 2 mL of culture medium per well. After cell attachment, pIgA1 was added to the experimental groups as follows: ① pGSN + pIgA1 + oe-NC group: HMCs transfected with the empty vector were cultured in DMEM complete medium containing 10 µg/mL plasma gelsolin and 1 mg/mL pIgA1; ② pGSN + pIgA1 + oe-*ADRB2* group: HMCs transfected with *ADRB2* overexpression plasmid were cultured in DMEM complete medium containing 10 µg/mL plasma gelsolin and 1 mg/mL pIgA1.

Prediction of Protein-protein Interactions

Amino acid sequences of GSN, IgA1, and ADRB2 were retrieved from the UniProt database. Complex structures of GSN–ADRB2 and IgA1–ADRB2 were predicted using AlphaFold3 in multimer mode. Predicted Template Modeling (pTM) scores and interface predicted Template Modeling (ipTM) scores were recorded to evaluate model confidence. Structural visualization and annotation of key interaction interfaces and amino acid residues were performed using PyMOL (version 3.1.6.1; Schrödinger, Inc. New York, NY, USA).

Data Statistics and Analysis

Experimental data are presented as the mean ± standard deviation (SD). Normality was assessed using the Shapiro–Wilk test, with $p > 0.05$ in all groups indicating no significant deviation from normal distribution. Homogeneity of variance was examined using Levene's and Bartlett's tests, which also yielded $p > 0.05$. Given that normality and homogeneity of variance assumptions were satisfied, independent samples *t*-tests were used for two-group comparisons, and one-way analysis of variance (ANOVA) was applied for comparisons across multiple groups. Following a significant omnibus *F*-test in one-way ANOVA, pairwise post hoc multiple comparisons were performed using Tukey's honestly significant difference (HSD) test to control family-wise error rate ($\alpha = 0.05$). Data analysis and figure construction were performed with GraphPad Prism 8.0.2 (GraphPad Software, San Diego, CA, USA). A *p*-value < 0.05 was considered statistically significant.

Results

pGSN Stimulation Upregulates TGF-β1 Expression in HMCs

To explore the effect of pGSN on glomerular fibrosis, we cultured HMCs *in vitro* and stimulated them with pGSN. The results demonstrated that *TGF-β1* mRNA ($p < 0.001$) (Fig. 1A) and protein ($p < 0.001$) (Fig. 1B) relative expression were significantly increased compared with the control group, indicating that pGSN stimulation markedly enhances *TGF-β1* expression, although the precise molecular mechanism remains unclear.

Transcriptomic Analysis of mRNA Expression Changes in HMCs After pGSN Stimulation

To investigate the mechanism underlying the increased *TGF-β1* expression after pGSN stimulation, we performed transcriptomic sequencing on pGSN-stimulated HMCs (48 hours) and normally cultured HMCs (n = 3 per group). Sequencing results showed that samples Q20, Q30, and GC contents of 97.55%–98.60%, 93.08%–95.94%, and 47.83%–50.06%, respectively, indicating high sequencing quality suitable for downstream analyses (**Supplementary Table 1**).

Screening criteria of $|\log_2 \text{FoldChange}| > 1$ and $p < 0.05$ identified 203 DEGs between control and pGSN groups, including 122 upregulated and 81 downregulated (Fig. 2A,B). The top 5 up- and downregulated DEGs are listed in **Supplementary Tables 2,3**. To validate sequencing reliability, three DEGs strongly associated with IgAN were selected for qPCR analysis. Results demonstrated consistent expression patterns between qPCR and sequencing, confirming the robustness and reproducibility of our transcriptomic dataset (Fig. 2C). GO and KEGG functional enrichment analyses were subsequently performed on the identified DEGs. Among these, the downregulated gene *ADRB2* has been reported to inhibit cellular fibrosis.

GO enrichment revealed that upregulated DEGs were significantly enriched in disease-related biological processes (BP), notably "response to virus" and "defense response to virus" (Fig. 2D). Downregulated DEGs were significantly enriched in "gas transport" (BP) and the "haptoglobin-hemoglobin complex" (cellular component, CC) (Fig. 2E).

KEGG pathway enrichment revealed that upregulated DEGs were primarily involved in the TGF-β signaling path-

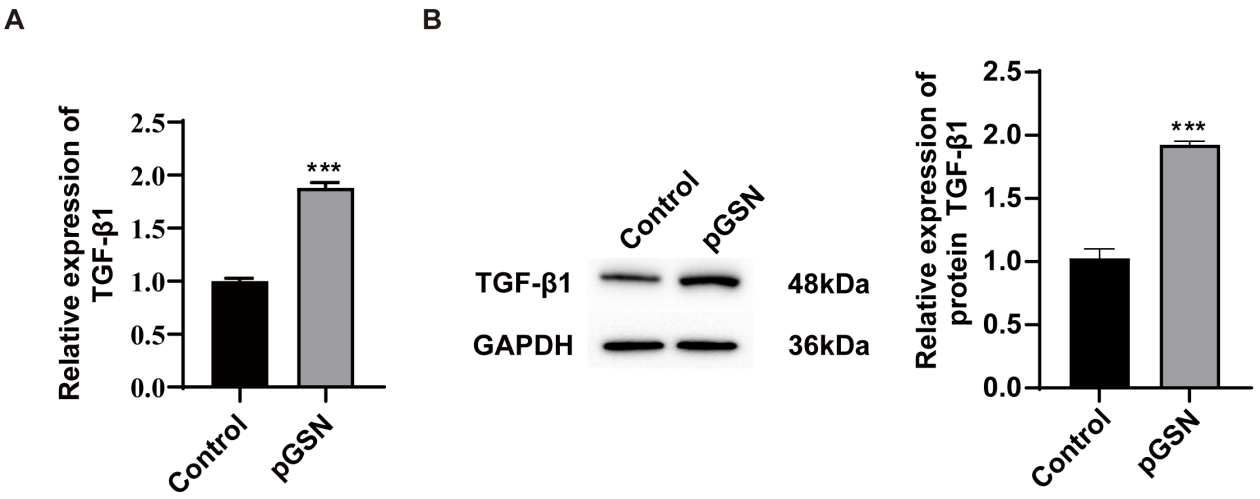

Fig. 1. Changes in TGF-β1 expression following pGSN stimulation. (A) Quantification of *TGF-β1* mRNA expression by quantitative polymerase chain reaction (qPCR). (B) Detection of *TGF-β1* protein expression by western blot (WB). Data are presented as mean ± SD (n = 3). ***$p < 0.001$.

way, as well as antiviral and inflammation-related pathways, including Toll-like receptor and NOD-like receptor signaling pathways (Fig. 2F). Notably, the cAMP signaling pathway, closely associated with fibrosis, was enriched in downregulated DEGs (Fig. 2G), consistent with its known protective role in IgA nephropathy. We therefore hypothesize that pGSN may contribute to glomerular fibrosis by modulating *ADRB2* expression and altering the cAMP signaling pathway. To validate this hypothesis, we performed functional studies of *ADRB2 in vitro*.

pGSN Promotes TGF-β1 Expression by Inhibiting ADRB2 Expression and cAMP Signaling Pathway Activation

To determine whether pGSN regulates glomerular fibrosis by modulating *ADRB2* expression, we overexpressed *ADRB2* in HMCs. Compared with the pGSN + oe-NC group, *ADRB2* mRNA ($p < 0.001$) and *ADRB2* protein ($p < 0.001$) levels were significantly elevated in the pGSN + oe-*ADRB2* group (Fig. 3A,D,E). Additionally, we assessed the expression of *PKA*, a core downstream of the cAMP signaling pathway. Compared with the control group, the pGSN group showed decreased *PKA* mRNA ($p < 0.001$) and *PKA* protein ($p < 0.001$) expression. In contrast, *PKA* mRNA ($p < 0.001$) and *PKA* protein ($p < 0.001$) levels in the pGSN + oe-*ADRB2* group were significantly higher than those in the pGSN + oe-NC group (Fig. 3B,D,E). The findings reveal that *ADRB2* overexpression reverses the suppression of the cAMP signaling pathway induced by pGSN stimulation.

We further examined changes in *TGF-β1* expression and the phosphorylation levels of *Smad2/3*. Compared with the control group, pGSN stimulation increased *TGF-β1* mRNA ($p < 0.001$) and *TGF-β1* protein ($p < 0.001$) levels, as well as enhanced phosphorylation of *Smad2/3* ($p < 0.001$). Conversely, *ADRB2* overexpression significantly reduced *TGF-β1* mRNA ($p < 0.001$), *TGF-β1* protein ($p < 0.001$), and Smad2/3 phosphorylation ($p < 0.01$) relative to the pGSN + oe-NC group (Fig. 3C,D,E). Immunofluorescence analysis demonstrated that pGSN stimulation significantly enhanced *TGF-β1* fluorescence intensity in HMCs ($p < 0.001$), whereas *ADRB2* overexpression notably reduced *TGF-β1* fluorescence intensity compared with the pGSN + oe-NC group ($p < 0.001$) (Fig. 3F). Collectively, these findings suggest that *ADRB2* overexpression activates the cAMP signaling pathway and suppresses *TGF-β1* expression, thereby exerting a regulatory role in glomerular fibrosis.

pGSN and pIgA1 Synergistically Promote TGF-β1 Expression via ADRB2/cAMP Signaling Suppression

To investigate the interaction between pIgA1, pGSN, and ADRB2, we performed molecular docking of ADRB2–GSN (ipTM = 0.69, pTM = 0.75) and ADRB2–IgA1 (ipTM = 0.72, pTM = 0.82) complexes to predict their potential binding sites. Based on these results, we validated the role of ADRB2 through cell-based experiments, transfecting HMCs with either an empty vector or an ADRB2 overexpression construct, followed by co-stimulation with pIgA1 and pGSN.

Docking analysis showed that ADRB2 can bind both GSN and IgA1 at distinct binding sites (Fig. 4A), supporting their cooperative regulation of the ADRB2 signaling pathway. qPCR and WB analyses demonstrated that, compared to the pGSN + pIgA1 + oe-NC group, the pGSN + pIgA1 + oe-ADRB2 group exhibited significantly increased ADRB2 mRNA ($p < 0.001$), ADRB2 protein ($p < 0.001$), *PKA* mRNA ($p < 0.01$), and *PKA* protein ($p < 0.001$)

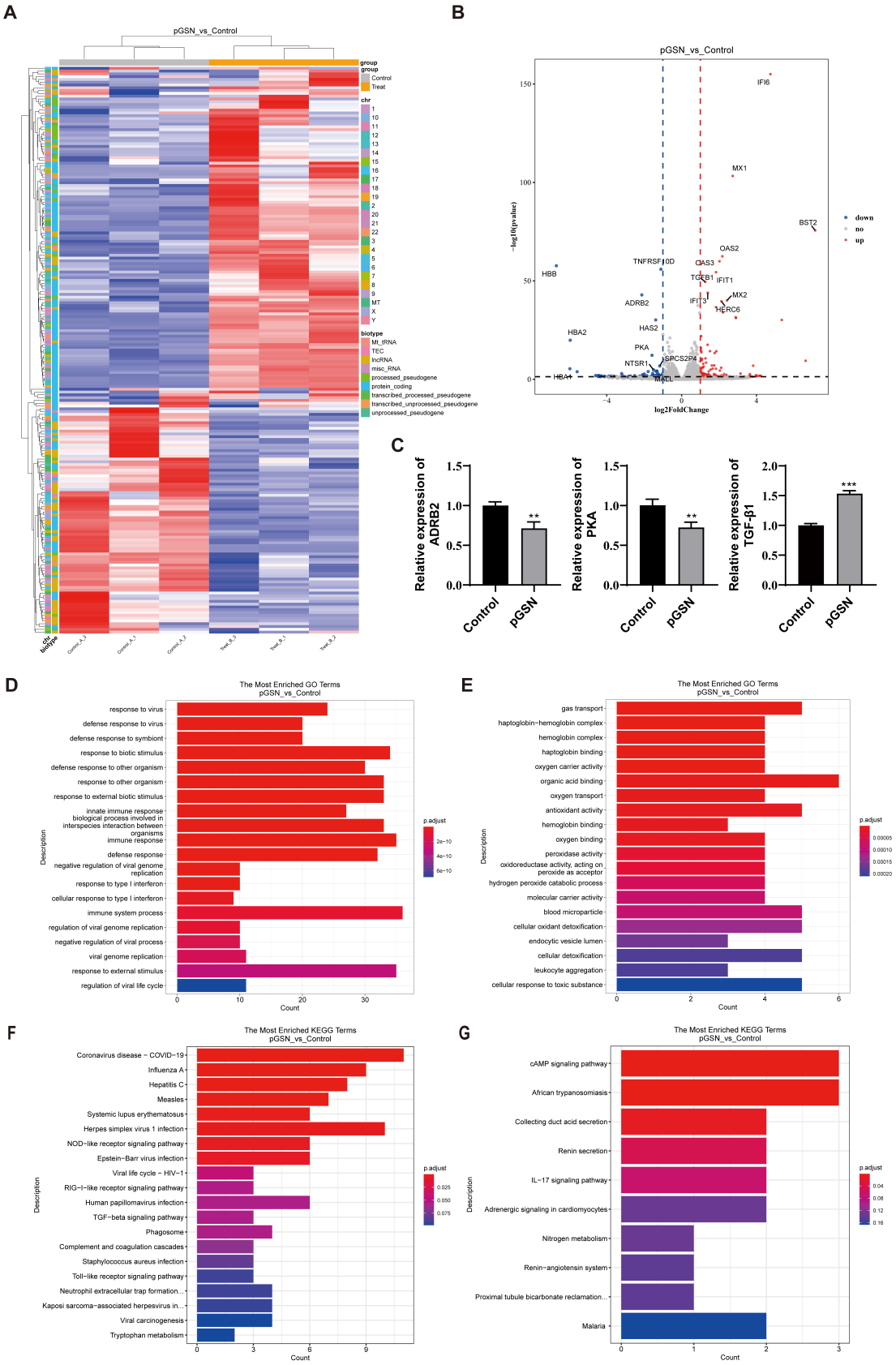

Fig. 2. Differential expression analysis and functional enrichment of transcriptome sequencing results were performed. (A) Heatmap of DEGs. (B) Volcano plot of DEGs. (C) qPCR validation of RNA-seq-identified DEGs (n = 3). (D) GO enrichment of upregulated DEGs. (E) GO enrichment of downregulated DEGs. (F) KEGG pathway enrichment of up-regulated DEGs. (G) KEGG pathway enrichment of downregulated DEGs. Data are presented as mean ± SD (n = 3). $^{**}p < 0.01$; $^{***}p < 0.001$.

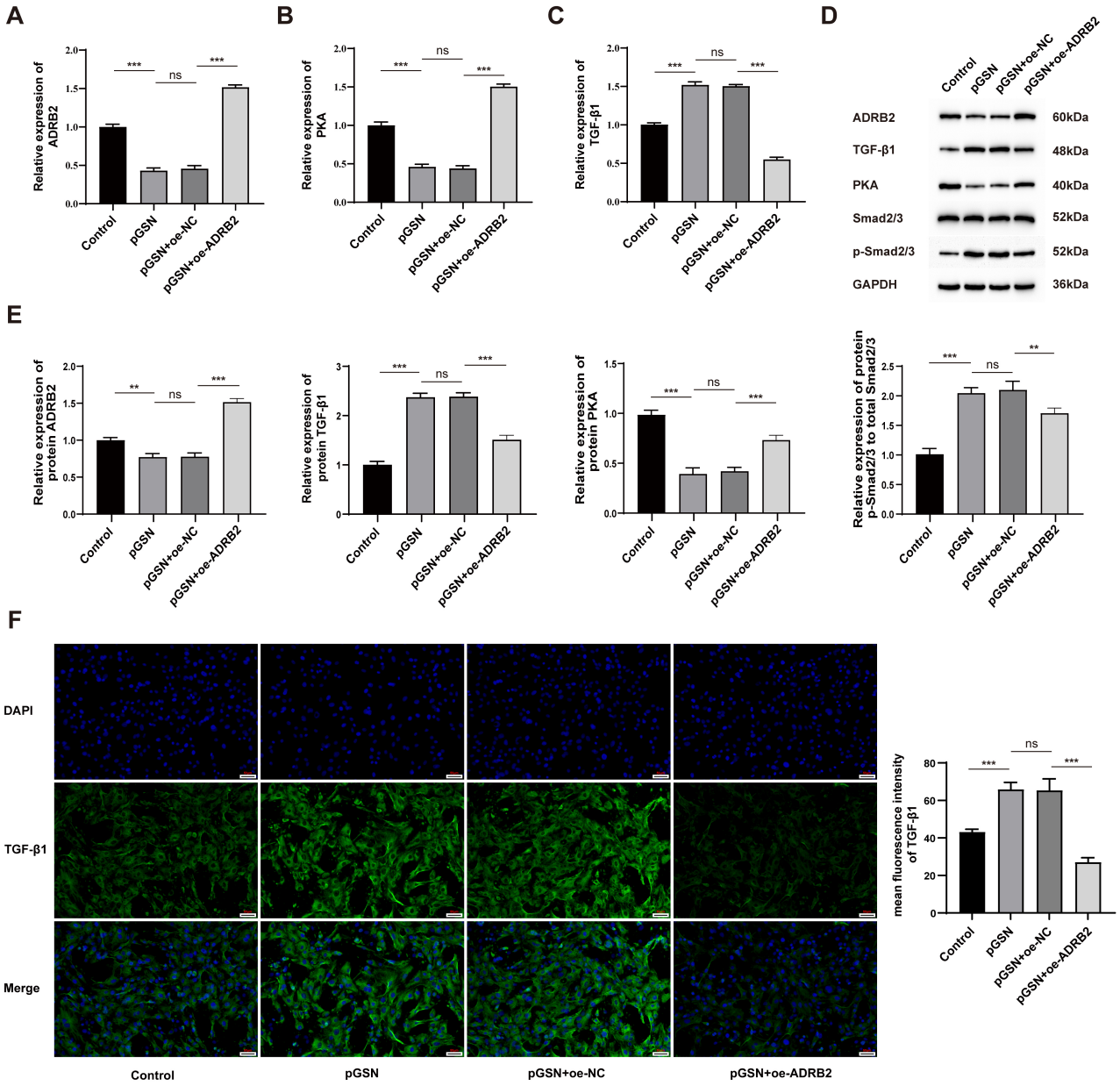

Fig. 3. qPCR, WB, and IF analysis of ADRB2, PKA, and TGF-β1 expression. (A–C) qPCR quantification of *ADRB2*, *PKA*, and *TGF-β1* mRNA levels. (D,E) WB detection of *ADRB2*, *PKA*, *Smad2/3*, p-*Smad2/3*, and *TGF-β1* protein expression. (F) Immunofluorescence (IF) analysis of the level of *TGF-β1* protein (200×, scale bar = 50 µm). Data are presented as mean ± SD (n = 3). $^{**}p < 0.01$; $^{***}p < 0.001$; ns, not significant.

(Fig. 4B,C,E). In contrast, *TGF-β1* mRNA ($p < 0.001$) and *TGF-β1* protein ($p < 0.001$) levels were significantly reduced (Fig. 4D,E). Immunofluorescence analysis further confirmed that *TGF-β1* fluorescence intensity was significantly lower in the pGSN + pIgA1 + oe-ADRB2 group compared with the pGSN + pIgA1 + oe-NC group ($p < 0.001$) (Fig. 4F). Together, these findings suggest that the pGSN and pIgA1 co-induced upregulation of *TGF-β1* is achieved through the inhibition of the ADRB2/cAMP signaling pathway.

Discussion

Glomerular fibrosis represents a critical event in the progression of multiple chronic kidney diseases toward ESRD, yet its underlying mechanisms remain complex and incompletely defined [30–32]. Our study reveals a previously unrecognized mechanism by which pGSN and pIgA1 synergistically inhibit the *ADRB2*/cAMP signaling axis, thereby promoting glomerular fibrosis. This discovery may offer a new theoretical foundation for understanding the pathogenesis of glomerular fibrosis and provide potential insights into therapeutic targets.

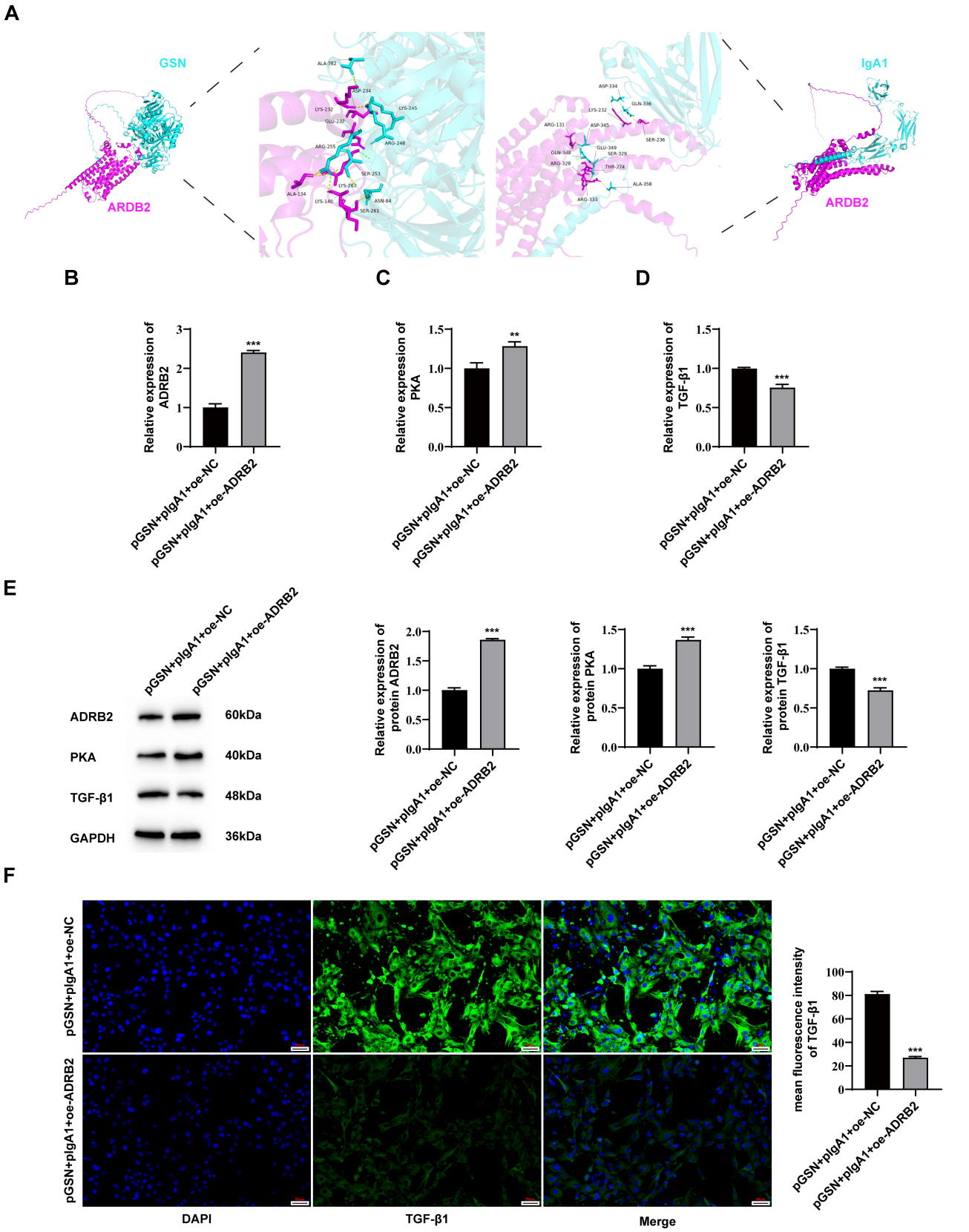

Fig. 4. Cooperative regulation of ADRB2, PKA, and TGF-β1 by pGSN and pIgA1. (A) Predicted binding sites of GSN, IgA1, and ADRB2. (B–D) qPCR analysis of *ADRB2*, *PKA*, and *TGF-β1* mRNA expression. (E) WB detection of *ADRB2*, *PKA*, and *TGF-β1* protein expression. (F) IF analysis of the expression level of *TGF-β1* protein (200×, scale bar = 50 μm). Data are presented as mean ± SD (n = 3). $^{**}p < 0.01$; $^{***}p < 0.001$.

pGSN, a secreted isoform of gelsolin, has recently been recognized as a multifunctional regulator in inflammatory responses [33], cardiovascular diseases [34], and hepatic disorders [35]. In IgAN patients, circulating pGSN levels are decreased, while glomerular pGSN accumulation is markedly elevated. This paradox can be explained by a dual-origin model: first, tissue injury releases extracellular F-actin, which binds avidly to circulating pGSN, leading to its entrapment within damaged glomeruli [36]; second, renal injury upregulates intrarenal pGSN expression [37]. Therefore, the combination of plasma-derived pGSN retention and enhanced endogenous renal pGSN expression collectively accounts for the simultaneous decrease in circulating pGSN and increase in glomerular pGSN accumulation. *In vitro* experiments have further demonstrated that pGSN upregulates *TGF-β1* expression in HMCs, thereby facilitating glomerular fibrosis [22,23]. To further elucidate the molecular mechanisms underlying pGSN-driven glomerular fibrosis, we performed transcriptomic sequencing of HMCs under both basal and pGSN-stimulated conditions.

Transcriptomic analysis revealed enrichment of the TGF-β signaling pathway among upregulated DEGs, consistent with our previous findings [23] and the pathological mechanisms of IgAN, where IgA immune complex deposition in glomeruli stimulates mesangial cells to upregulate *TGF-β1* mRNA expression, driving sustained activation of the TGF-β/Smad signaling pathway [38]. Persistent activation promotes mesangial proliferation and excessive accumulation of extracellular matrix (ECM), resulting in glomerulosclerosis and tubulointerstitial fibrosis, ultimately worsening proteinuria and contributing to further decline in renal function [39]. Additionally, the cAMP signaling pathway was significantly enriched among downregulated DEGs. cAMP inhibits fibroblast proliferation and EMT, thereby limiting abnormal ECM deposition and preventing glomerulosclerosis and tubulointerstitial fibrosis [40]. Mechanistically, cAMP activates *PKA*, which phosphorylates cAMP responsive element binding protein 1 (CREB) to upregulate transforming growth factor beta-induced factor 1 (TGIF1). TGIF1 suppresses TGF-β1/Smad signaling by binding the activated *Smad2/3* complex and recruiting histone deacetylases, forming a negative feedback loop [41]. Notably, *in vitro* administration of cAMP agonists has been shown to reduce *TGF-β1* protein expression in cardiomyocytes and alleviate cardiac fibrosis in mice. In addition, cAMP signaling inhibits *TGF-β1* production across various cell types while suppressing fibrotic processes [42]. Therefore, the cAMP signaling pathway may also be critically implicated in the regulation of glomerular fibrosis in IgAN patients.

In addition, the pathway gene *ADRB2* attracted our attention. Previous studies have shown that *ADRB2* protein is highly expressed on the membranes of fibroblasts and keratinocytes, where it primarily functions in inhibiting inflammation and promoting reepithelization, and is associated with abnormal wound healing [43,44]. Wan *et al.* [27] reported that the *ADRB2* expression is reduced in pulmonary fibrosis samples, and mechanistic analyses revealed that *ADRB2* regulates fibroblast differentiation through the TGF-β/Smad signaling pathway. Furthermore, *ADRB2* has been shown to ameliorate bladder fibrosis [28] and modulate the activity of human dermal fibroblasts [29].

In our study, pGSN stimulation downregulated *ADRB2* expression, while *ADRB2* overexpression reduced *TGF-β1* levels. We propose that pGSN may inhibit *ADRB2* through several mechanisms: regulation of epigenetic modifying enzymes that alter methylation status or histone modifications at the *ADRB2* promoter region; upregulation of specific miRNAs (e.g., let-7) that guide the RISC complex to target the *ADRB2* 3'UTR for post-transcriptional regulation [45]; or activation of E3 ubiquitin ligases that promote *ADRB2* protein ubiquitination and degradation [46]. Collectively, these findings suggest that pGSN stimulation in HMCs suppresses *ADRB2* expression, thereby enhancing *TGF-β1* production and promoting glomerular fibrosis.

IgA is the most abundant immunoglobulin in humans and consists of IgA1 and IgA2 subtypes. Growing evidence underscores the critical role of galactose-deficient IgA1 (Gd-IgA1) in the pathogenesis of IgAN. Elevated plasma concentrations of Gd-IgA1 are significantly positively correlated with increased risk of progression to ESKD in patients with IgAN [47]. Mechanistic studies reveal that both pIgA1 and mIgA1 isolated from patient sera induce dose-dependent upregulation of renin and *TGF-β1* gene expression in HMCs [48]. Furthermore, IgA1-containing immune complexes from pediatric IgAN patients significantly enhance laminin secretion and proliferative activity in HMCs upon stimulation [49]. Our previous experiments confirmed these findings, demonstrating that pIgA1 stimulation not only promotes HMCs proliferation but also elevates *TGF-β1* secretion. Notably, pGSN exerts synergistic effects with pIgA1 in driving these pathological responses [23].

Notably, *ADRB2* overexpression reverses the *TGF-β1* upregulation and subsequent fibrotic processes induced by synergistic stimulation with pGSN and pIgA1, highlighting its therapeutic potential in glomerular fibrosis. Based on this potential, salmeterol, a selective long-acting β2-adrenergic agonist [50], emerges as a promising candidate therapy for IgAN. Although inhaled administration results in low systemic exposure with limited direct renal effects, we plan to evaluate its capacity to alter renal phenotypes through optimized low-dose inhaled regimens. Additionally, kidney-targeted delivery approaches will be explored to enhance renal uptake while minimizing systemic adverse effects.

This study revealed that pGSN and pIgA1 synergistically promote *TGF-β1* expression primarily through the *ADRB2*/cAMP signaling pathway (Fig. 5). However, these

findings are currently limited to the cellular level and therefore cannot fully capture the complex immune, hemodynamic, and microenvironmental context of IgAN *in vivo*. To address this limitation, our next phase of research will validate the key findings in IgAN animal models. Specifically, we plan to: (1) induce or utilize spontaneous IgAN models and administer pGSN-targeted interventions, (2) quantify renal functional parameters, (3) conduct renal histopathological assessments, and (4) evaluate renal expression and activation of the *TGF-β1*/*ADRB2*/*PKA* axis at the tissue level. These *in vivo* studies will determine whether the mechanisms identified in cultured HMCs translate into relevant phenotypes and therapeutic targets.

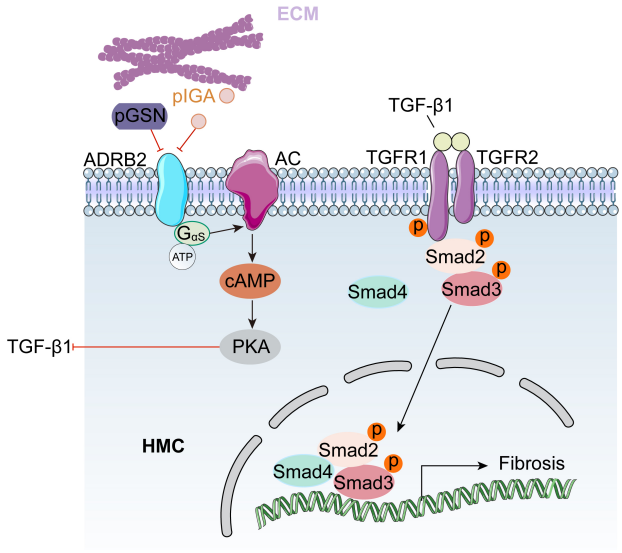

Fig. 5. Proposed mechanism by which pGSN and pIgA synergistically regulate ADRB2-mediated HMCs fibrosis. During the pathogenesis of IgA nephropathy, pGSN and pIgA1 accumulate in the glomerular mesangium, where local concentrations increase. Their synergistic action downregulates *ADRB2* expression in HMCs, suppressing cAMP/*PKA* signaling activity and reducing the inhibition of *TGF-β1*. Elevated *TGF-β1* activates the TGF-β/Smad pathway, enhancing transcription of fibrosis-related genes and promoting glomerular fibrosis.

Moreover, glomerular fibrosis represents a critical event in the progression of diverse chronic kidney diseases toward ESRD, typically accompanied by tubulointerstitial injury. Notably, pGSN and pIgA1 deposits are predominantly localized within the glomeruli, with only minimal deposition observed in the renal tubules. The mechanisms by which glomerular deposition of pGSN and IgA1 subsequently initiates tubulointerstitial damage, ultimately culminating in ESRD, remain to be elucidated.

Conclusion

This study demonstrates that pGSN promotes *TGF-β1* expression in HMCs by inhibiting the *ADRB2*/cAMP signaling pathway. These findings reveal a novel molecular mechanism underlying pGSN-induced glomerular fibrosis, and provide both a theoretical framework and potential therapeutic targets for intervention in this pathological process.

Availability of Data and Materials

The raw RNA-sequencing data reported in this study have been deposited in the China National Center for Bioinformation (https://www.cncb.ac.cn/) under accession number HRA012881.

Author Contributions

CSH conceived, designed, and conducted the experiments, as well as drafting the initial manuscript. YJC, KW, CLC and MY analyzed and interpreted the data. CHS designed the study, performed formal analysis, contributed to writing, reviewing, and editing, and provided supervision. All authors contributed to critical revision of the manuscript for important intellectual content. All authors read and approved the final manuscript. All authors have participated sufficiently in the work and agreed to be accountable for all aspects of the work.

Ethics Approval and Consent to Participate

The research protocol was reviewed and approved by the Ethics Committee of Guizhou University of Traditional Chinese Medicine (Approval No. KS2022-10). All procedures involving human participants were performed in compliance with the Declaration of Helsinki and the CIOMS International Ethical Guidelines. All participants provided informed consent by signing an informed consent form.

Acknowledgment

Not applicable.

Funding

This work was sponsored by the National Natural Science Foundation of China (grant number: 82260144).

Conflict of Interest

The authors declare no conflict of interest.

Supplementary Material

Supplementary material associated with this article can be found, in the online version, at https://doi.org/10.24976/Discov.Med.202537202.221.

References

[1] Pattrapornpisut P, Avila-Casado C, Reich HN. IgA Nephropathy: Core Curriculum 2021. American Journal of Kidney Diseases: the Official Journal of the National Kidney Foundation. 2021; 78: 429–441. https://doi.org/10.1053/j.ajkd.2021.01.024.

[2] Nihei Y, Suzuki H, Suzuki Y. Current understanding of IgA antibodies in the pathogenesis of IgA nephropathy. Frontiers in Immunology. 2023; 14: 1165394. https://doi.org/10.3389/fimmu.2023.1165394.

[3] Walsh M, Sar A, Lee D, Yilmaz S, Benediktsson H, Manns B, *et al*. Histopathologic features aid in predicting risk for progression of IgA nephropathy. Clinical Journal of the American Society of Nephrology: CJASN. 2010; 5: 425–430. https://doi.org/10.2215/CJN.06530909.

[4] Peng W, Tang Y, Tan L, Qin W. Crescents and Global Glomerulosclerosis in Chinese IgA Nephropathy Patients: A Five-Year Follow-Up. Kidney & Blood Pressure Research. 2019; 44: 103–112. https://doi.org/10.1159/000498874.

[5] Chung CS, Lee JH, Jang SH, Cho NJ, Kim WJ, Heo NH, *et al*. Age-adjusted global glomerulosclerosis predicts renal progression more accurately in patients with IgA nephropathy. Scientific Reports. 2020; 10: 6270. https://doi.org/10.1038/s41598-020-63366-0.

[6] Working Group of the International IgA Nephropathy Network and the Renal Pathology Society, Cattran DC, Coppo R, Cook HT, Feehally J, Roberts IS, *et al*. The Oxford classification of IgA nephropathy: rationale, clinicopathological correlations, and classification. Kidney International. 2009; 76: 534–545. https://doi.org/10.1038/ki.2009.243.

[7] Trimarchi H, Barratt J, Cattran DC, Cook HT, Coppo R, Haas M, *et al*. Oxford Classification of IgA nephropathy 2016: an update from the IgA Nephropathy Classification Working Group. Kidney International. 2017; 91: 1014–1021. https://doi.org/10.1016/j.kint.2017.02.003.

[8] Huang R, Fu P, Ma L. Kidney fibrosis: from mechanisms to therapeutic medicines. Signal Transduction and Targeted Therapy. 2023; 8: 129. https://doi.org/10.1038/s41392-023-01379-7.

[9] Gui Z, Suo C, Wang Z, Zheng M, Fei S, Chen H, *et al*. Impaired ATG16L-Dependent Autophagy Promotes Renal Interstitial Fibrosis in Chronic Renal Graft Dysfunction Through Inducing EndMT by NF-κB Signal Pathway. Frontiers in Immunology. 2021; 12: 650424. https://doi.org/10.3389/fimmu.2021.650424.

[10] Hu L, Ding M, He W. Emerging Therapeutic Strategies for Attenuating Tubular EMT and Kidney Fibrosis by Targeting Wnt/β-Catenin Signaling. Frontiers in Pharmacology. 2022; 12: 830340. https://doi.org/10.3389/fphar.2021.830340.

[11] Ma J, van der Zon G, Sanchez-Duffhues G, Ten Dijke P. TGF-β-mediated Endothelial to Mesenchymal Transition (EndMT) and the Functional Assessment of EndMT Effectors using CRISPR/Cas9 Gene Editing. Journal of Visualized Experiments: JoVE. 2021; 10.3791/62198. https://doi.org/10.3791/62198.

[12] Böttinger EP. TGF-beta in renal injury and disease. Seminars in Nephrology. 2007; 27: 309–320. https://doi.org/10.1016/j.semnephrol.2007.02.009.

[13] Böttinger EP, Bitzer M. TGF-beta signaling in renal disease. Journal of the American Society of Nephrology: JASN. 2002; 13: 2600–2610. https://doi.org/10.1097/01.asn.0000033611.79556.ae.

[14] Yin HL, Stossel TP. Control of cytoplasmic actin gel-sol transformation by gelsolin, a calcium-dependent regulatory protein. Nature. 1979; 281: 583–586. https://doi.org/10.1038/281583a0.

[15] Osborn TM, Verdrengh M, Stossel TP, Tarkowski A, Bokarewa M. Decreased levels of the gelsolin plasma isoform in patients with rheumatoid arthritis. Arthritis Research & Therapy. 2008; 10: R117. https://doi.org/10.1186/ar2520.

[16] Christofidou-Solomidou M, Scherpereel A, Solomides CC, Muzykantov VR, Machtay M, Albelda SM, *et al*. Changes in plasma gelsolin concentration during acute oxidant lung injury in mice. Lung. 2002; 180: 91–104. https://doi.org/10.1007/s004080000084.

[17] DiNubile MJ, Stossel TP, Ljunghusen OC, Ferrara JLM, Antin JH. Prognostic implications of declining plasma gelsolin levels after allogeneic stem cell transplantation. Blood. 2002; 100: 4367–4371. https://doi.org/10.1182/blood-2002-06-1672.

[18] Mounzer KC, Moncure M, Smith YR, Dinubile MJ. Relationship of admission plasma gelsolin levels to clinical outcomes in patients after major trauma. American Journal of Respiratory and Critical Care Medicine. 1999; 160: 1673–1681. https://doi.org/10.1164/ajrccm.160.5.9807137.

[19] Piktel E, Levental I, Durnaś B, Janmey PA, Bucki R. Plasma Gelsolin: Indicator of Inflammation and Its Potential as a Diagnostic Tool and Therapeutic Target. International Journal of Molecular Sciences. 2018; 19: 2516. https://doi.org/10.3390/ijms19092516.

[20] Rothenbach PA, Dahl B, Schwartz JJ, O'Keefe GE, Yamamoto M, Lee WM, *et al*. Recombinant plasma gelsolin infusion attenuates burn-induced pulmonary microvascular dysfunction. Journal of Applied Physiology (Bethesda, Md.: 1985). 2004; 96: 25–31. https://doi.org/10.1152/japplphysiol.01074.2002.

[21] Suhler E, Lin W, Yin HL, Lee WM. Decreased plasma gelsolin concentrations in acute liver failure, myocardial infarction, septic shock, and myonecrosis. Critical Care Medicine. 1997; 25: 594–598. https://doi.org/10.1097/00003246-199704000-00007.

[22] Han C, Zhang L, Zhu X, Tang J, Jin X. Plasma gelsolin levels are decreased and correlate with fibrosis in IgA nephropathy. Experimental Biology and Medicine (Maywood, N.J.). 2013; 238: 1318–1327. https://doi.org/10.1177/1535370213503256.

[23] Zhang L, Han C, Ye F, He Y, Jin Y, Wang T, *et al*. Plasma Gelsolin Induced Glomerular Fibrosis via the TGF-β1/Smads Signal Transduction Pathway in IgA Nephropathy. International Journal of Molecular Sciences. 2017; 18: 390. https://doi.org/10.3390/ijms18020390.

[24] Poncelet AC, de Caestecker MP, Schnaper HW. The transforming growth factor-beta/SMAD signaling pathway is present and functional in human mesangial cells. Kidney International. 1999; 56: 1354–1365. https://doi.org/10.1046/j.1523-1755.1999.00680.x.

[25] Chen R, Huang C, Morinelli TA, Trojanowska M, Paul RV. Blockade of the effects of TGF-beta1 on mesangial cells by overexpression of Smad7. Journal of the American Society of Nephrology: JASN. 2002; 13: 887–893. https://doi.org/10.1681/ASN.V134887.

[26] Zhou P, Wan X, Zou Y, Chen Z, Zhong A. Transforming growth factor beta (TGF-β) is activated by the CtBP2-p300-AP1 transcriptional complex in chronic renal failure. International Journal of Biological Sciences. 2020; 16: 204–215. https://doi.org/10.7150/ijbs.38841.

[27] Wan R, Wang L, Duan Y, Zhu M, Li W, Zhao M, *et al*. ADRB2 inhibition combined with antioxidant treatment alleviates lung fibrosis by attenuating TGFβ/SMAD signaling in lung fibroblasts. Cell Death Discovery. 2023; 9: 407. https://doi.org/10.1038/s41420-023-01702-9.

[28] Lai J, Chen G, Su H, He Q, Xiao K, Liao B, *et al*. β-Adrenoceptor Signaling Activation Improves Bladder Fibrosis by Inhibiting Extracellular Matrix Deposition of Bladder Outlet Obstruction. Frontiers in Bioscience (Landmark Edition). 2024; 29: 336. https://doi.org/10.31083/j.fbl2909336.

[29] Le Provost GS, Pullar CE. β2-adrenoceptor activation modulates skin wound healing processes to reduce scarring. The Journal of Investigative Dermatology. 2015; 135: 279–288. https://doi.org/10.1038/jid.2014.312.

[30] Kim HW, Park JT, Joo YS, Kang SC, Lee JY, Lee S, *et al*. Systolic blood pressure and chronic kidney disease progression in patients with primary glomerular disease. Journal of Nephrology. 2021; 34: 1057–1067. https://doi.org/10.1007/s40620-020-00930-x.

[31] Altintas MM, Agarwal S, Sudhini Y, Zhu K, Wei C, Reiser J. Pathogenesis of Focal Segmental Glomerulosclerosis and Related Disorders. Annual Review of Pathology. 2025; 20: 329–353. https://doi.org/10.1146/annurev-pathol-051220-092001.

[32] Coresh J, Turin TC, Matsushita K, Sang Y, Ballew SH, Appel LJ, *et al*. Decline in estimated glomerular filtration rate and subsequent risk of end-stage renal disease and mortality. JAMA. 2014; 311: 2518–2531. https://doi.org/10.1001/jama.2014.6634.

[33] Bucki R, Georges PC, Espinassous Q, Funaki M, Pastore JJ, Chaby R, *et al*. Inactivation of endotoxin by human plasma gelsolin. Biochemistry. 2005; 44: 9590–9597. https://doi.org/10.1021/bi0503504.

[34] Pan JW, He LN, Xiao F, Shen J, Zhan RY. Plasma gelsolin levels and outcomes after aneurysmal subarachnoid hemorrhage. Critical Care (London, England). 2013; 17: R149. https://doi.org/10.1186/cc12828.

[35] Cheng Y, Hu X, Liu C, Chen M, Wang J, Wang M, *et al*. Gelsolin Inhibits the Inflammatory Process Induced by LPS. Cellular Physiology and Biochemistry: International Journal of Experimental Cellular Physiology, Biochemistry, and Pharmacology. 2017; 41: 205–212. https://doi.org/10.1159/000456043.

[36] Lee WM, Galbraith RM. The extracellular actin-scavenger system and actin toxicity. The New England Journal of Medicine. 1992; 326: 1335–1341. https://doi.org/10.1056/NEJM199205143262006.

[37] Yu CJ, Damaiyanti DW, Yan SJ, Wu CH, Tang MJ, Shieh DB, *et al*. The Pathophysiologic Role of Gelsolin in Chronic Kidney Disease: Focus on Podocytes. International Journal of Molecular Sciences. 2021; 22: 13281. https://doi.org/10.3390/ijms222413281.

[38] Han SY, Ihm CG, Cha DR, Kang YS, Han KH, Kim HK, *et al*. Effect of IgA aggregates on transforming growth factor-beta1 production in human mesangial cells and the intraglomerular expression of transforming growth factor-beta1 in patients with IgA nephropathy. The Korean Journal of Internal Medicine. 2005; 20: 40–47. https://doi.org/10.3904/kjim.2005.20.1.40.

[39] Wu W, Jiang XY, Zhang QL, Mo Y, Sun LZ, Chen SM. Expression and significance of TGF-beta1/Smad signaling pathway in children with IgA nephropathy. World Journal of Pediatrics: WJP. 2009; 5: 211–215. https://doi.org/10.1007/s12519-009-0040-3.

[40] Insel PA, Murray F, Yokoyama U, Romano S, Yun H, Brown L, *et al*. cAMP and Epac in the regulation of tissue fibrosis. British Journal of Pharmacology. 2012; 166: 447–456. https://doi.org/10.1111/j.1476-5381.2012.01847.x.

[41] Meng L, Lu Y, Wang X, Cheng C, Xue F, Xie L, *et al*. NPRC deletion attenuates cardiac fibrosis in diabetic mice by activating PKA/PKG and inhibiting TGF-β1/Smad pathways. Science Advances. 2023; 9: eadd4222. https://doi.org/10.1126/sciadv.add4222.

[42] Liu X, Sun SQ, Hassid A, Ostrom RS. cAMP inhibits transforming growth factor-beta-stimulated collagen synthesis via inhibition of extracellular signal-regulated kinase 1/2 and Smad signaling in cardiac fibroblasts. Molecular Pharmacology. 2006; 70: 1992–2003. https://doi.org/10.1124/mol.106.028951.

[43] Ten Hove AS, Mallesh S, Zafeiropoulou K, de Kleer JWM, van Hamersveld PHP, Welting O, *et al*. Sympathetic activity regulates epithelial proliferation and wound healing via adrenergic receptor α_2A. Scientific Reports. 2023; 13: 17990. https://doi.org/10.1038/s41598-023-45160-w.

[44] Huo J, Sun S, Geng Z, Sheng W, Chen R, Ma K, *et al*. Bone Marrow-Derived Mesenchymal Stem Cells Promoted Cutaneous Wound Healing by Regulating Keratinocyte Migration via β_2-Adrenergic Receptor Signaling. Molecular Pharmaceutics. 2018; 15: 2513–2527. https://doi.org/10.1021/acs.molpharmaceut.7b01138.

[45] Wang WCH, Juan AH, Panebra A, Liggett SB. MicroRNA let-7 establishes expression of beta2-adrenergic receptors and dynamically down-regulates agonist-promoted down-regulation. Proceedings of the National Academy of Sciences of the United States of America. 2011; 108: 6246–6251. https://doi.org/10.1073/pnas.1101439108.

[46] Han SO, Xiao K, Kim J, Wu JH, Wisler JW, Nakamura N, *et al*. MARCH2 promotes endocytosis and lysosomal sorting of carvedilol-bound β(2)-adrenergic receptors. The Journal of Cell Biology. 2012; 199: 817–830. https://doi.org/10.1083/jcb.201208192.

[47] Chen P, Yu G, Zhang X, Xie X, Wang J, Shi S, *et al*. Plasma Galactose-Deficient IgA1 and C3 and CKD Progression in IgA Nephropathy. Clinical Journal of the American Society of Nephrology: CJASN. 2019; 14: 1458–1465. https://doi.org/10.2215/CJN.13711118.

[48] Lai KN, Tang SCW, Guh JY, Chuang TD, Lam MF, Chan LYY, *et al*. Polymeric IgA1 from patients with IgA nephropathy upregulates transforming growth factor-beta synthesis and signal transduction in human mesangial cells via the renin-angiotensin system. Journal of the American Society of Nephrology: JASN. 2003; 14: 3127–3137. https://doi.org/10.1097/01.asn.0000095639.56212.bf.

[49] Novak J, Raskova Kafkova L, Suzuki H, Tomana M, Matousovic K, Brown R, *et al*. IgA1 immune complexes from pediatric patients with IgA nephropathy activate cultured human mesangial cells. Nephrology, Dialysis, Transplantation: Official Publication of the European Dialysis and Transplant Association - European Renal Association. 2011; 26: 3451–3457. https://doi.org/10.1093/ndt/gfr448.

[50] Johnson M, Butchers PR, Coleman RA, Nials AT, Strong P, Sumner MJ, *et al*. The pharmacology of salmeterol. Life Sciences. 1993; 52: 2131–2143. https://doi.org/10.1016/0024-3205(93)90728-l.